Kossel diffraction observed with X-ray color camera during PIXE of nano-scale periodic multilayer

Meiyi Wu[1,2], Karine Le Guen[1,2], Jean-Michel André[1,2], Philippe Jonnard[1,2], Ian Vickridge[3,4], Didier Schmaus[3,4], Emrick Briand[3,4], Philippe Walter[5,6], Qiushi Huang[7], Zhanshan Wang[7]

[1] *Sorbonne Universités, UPMC Univ Paris 06, Laboratoire de Chimie Physique - Matière et Rayonnement, boîte courier 1140, 4 Place Jussieu, F-75252 Paris cedex 05, France*

[2] *CNRS UMR 7614, Laboratoire de Chimie Physique - Matière et Rayonnement, boîte courier 1140, 4 Place Jussieu, F-75252 Paris cedex 05, France.*

[3] *Sorbonne Universités, UPMC Univ Paris 06, Institut des NanoSciences de Paris, 4 place Jussieu, boîte courrier 840, F-75252 Paris cedex 05, France*

[4] *CNRS UMR 7588, Institut des NanoSciences de Paris, 4 place Jussieu, boîte courrier 840, F-75252 Paris cedex 05, France*

[5] *Sorbonne Universités, UPMC Univ Paris 06, Laboratoire d'Archéologie Moléculaire et Structurale, 4 place Jussieu, 75005 Paris, France*

[6] *CNRS, UMR 8220, Laboratoire d'Archéologie Moléculaire et Structurale, 4 place Jussieu, 75005 Paris, France*

[7] *Key Laboratory of Advanced Micro-Structured Materials, Institute of Precision Optical Engineering, School of Physics Science and Engineering, Tongji University, Shanghai 200092, China*

Key words: PIXE, periodic multilayer, Kossel diffraction.

Abstract

By combining Kossel diffraction with particle induced X-ray emission, we have developed a new methodology to analyze nano-scale thin films. We report the Kossel diffraction generated by irradiating Pd/Y based nano-scale periodic multilayers with 2 MeV protons. The intensity of characteristic Pd Lα X-ray emission is measured as a function of the detection angle (grazing exit). An oscillation of its intensity is observed when the detection angle varies around the Bragg angle, which corresponds to the energy of the emission and the period of the multilayer. Use of the X-ray color camera enables the whole setup to be fixed so that no angular scan is required, greatly simplifying the experimental condition. From the features of the Kossel curves, we are able to deduce that nitrided Pd/Y multilayers exhibit much less layer intermixing than the non-nitrided multilayers. The experimental results show that it is possible to distinguish by the shape of Kossel curves of multilayers with B_4C barrier layers located in different interfaces. This demonstrates that Kossel diffraction is structural sensitive.

Introduction

The Kossel process refers to the interference of characteristic X-rays generated within and scattered by the atoms present within a periodic micro-structure. Typical diffraction patterns are formed around the Bragg angle corresponding to the wavelength (or energy) of the emission and the period of the lattice. In 1935, Walther Kossel experimentally demonstrated such interferences for a crystalline structure [1]. The phenomenon was then named after him as "Kossel effect". Its observation requires two essential factors: first, the ionization of a core level in order to produce the characteristic emission; second, a periodic structure to diffract the emitted X-ray. The source for the ionization can

vary. It can be X-ray provided either by an X-ray tube [2-4] or by synchrotron radiation [5-8], energetic electrons [9-12] or energetic charged particles (protons or ions) [13-19] as we report in this paper.

Studies of both crystals and interferential multilayers using various techniques have been widely reported, but it was not until our previous paper [20] that the study of periodic multilayer by Kossel diffraction of X-rays generated by proton beam was first reported. We successfully observed the Kossel curves of Cr Kα and Sc Kα emissions of a Cr/B_4C/Sc periodic multilayer irradiated by 2 MeV protons. However due to the very small solid angle of the highly collimated detector the counting statistics were not ideal even for long acquisition times, and we mentioned in our conclusion that it might be improved by using an X-ray color camera, that is a CCD camera in which each pixel can provide an energy-dispersed X-ray emission spectrum. This allows us to avoid the angular scans in our measurements, thus reducing the overall acquisition time while allowing an improvement of statistics.

The work presented in this paper focuses on the Pd/Y based multilayers, which are designed as reflecting mirrors to work in the 7.5-11 nm wavelength range. Derivative systems are also designed with the motivation of improving the optical performance of the reflecting mirror owing to more abrupt interfaces.

Experimental details

Samples are deposited onto sliced and polished Si (100) wafers by using DC magnetron sputtering. The originally designed structure is B_4C(2.5 nm)/[Pd(2 nm)/Y(2 nm)]$_{\times 40}$/Si. The B_4C capping layer is added to protect the samples against oxidation. A series of samples is fabricated with 0-6% of nitrogen gas N_2 in the sputtering gas instead of pure argon because we believe that the formation of YN will help improve the thermal stability of the sample and reduce the interdiffusion between Pd and Y layers [21,22]. Another series of samples has B_4C barrier layers inserted at Pd-on-Y, Y-on-Pd or both interfaces in order to prevent or reduce the interdiffusion between the Pd and Y layers [23]. The thickness of the barrier layers is 1 nm. The physical structures of the samples, including thickness and roughness of each layer are determined by grazing incident X-ray reflectometry immediately following the deposition process.

The proton beam is generated by the Van de Graaff accelerator of the SAFIR (Système d'Analyse par Faisceaux d'Ions Rapides) platform. The proton energy is set at 2.0 MeV, which is suitable to ionize the Pd atoms in their L shell uniformly through the whole multilayer. The energy loss of the proton beam is only about 0.5% after penetrating the multilayer whose total thickness is approximately 200 nm. The X-ray color camera is an iKon-M from Andor Technologies equipped with a 1024×1024 sensor array with 13×13 μm pixels. Instead of using the native spatial resolution, we select a 4×4 binning leading to a resolution of 256×256. Such selection improves the energy resolution by minimizing the charge sharing effect between adjacent pixels while still providing adequate angular resolution. It also simplifies the data treatment by reducing the size of data files. The camera spans an angular range of 2.7° corresponding to 256 horizontal pixels in Fig. 1.

For a given X-ray emission, we measure its intensity as a function of the detection angle with the X-ray color camera while irradiating the sample with the proton beam. The experimental setup is schematically presented in Fig. 1 where the X-ray color camera is placed perpendicular to the incident proton beam with a 200 μm beryllium film to filter the scattered protons. The experimentally obtained image of particle induced X-ray emission (PIXE) presented in Fig. 1 is the spatial distribution of total X-ray intensity on the detected area for B_4C(2.5 nm)/[Pd(2 nm)/B_4C(2 nm)/Y(2 nm)]$_{\times 40}$/Si multilayer obtained after a 2 hour irradiation with about 35 nA of 2 MeV protons in a 2 mm beam spot. This

corresponds to about 5×10^{16} protons cm^{-2}. The Kossel feature cannot be observed on this image yet. It requires further treatment, which will be explained later, to be extracted from this image.

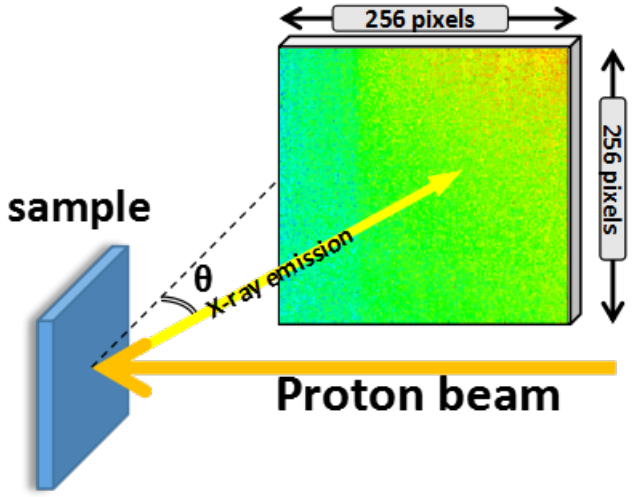

Fig. 1. Geometry of the experimental setup. θ is the detection angle. The presented experimental image is the spatial distribution of total X-ray intensity on the detector array for B_4C(2.5 nm)/[Pd(2 nm)/B_4C(2 nm)/Y(2 nm)]$_{\times40}$/Si multilayer irradiated as described in the text.

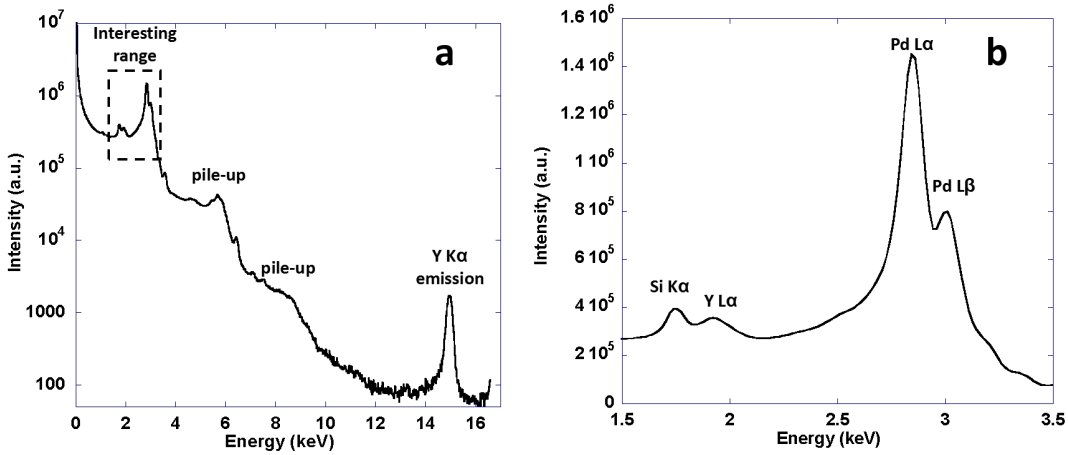

Fig. 2. Spectrum of B_4C(2.5 nm)/[Pd(2 nm)/B_4C(2 nm)/Y(2 nm)]$_{\times40}$/Si multilayer: a) overview, intensity in log scale; b) zoomed range of interest, intensity in linear scale.

Note that a complete X-ray spectrum is recorded by each pixel of the X-ray color camera. To identify the emission peaks, we sum the spectra recorded by all pixels in order to get more reliable statistics. An overview (intensity in log scale) of the summed X-ray spectrum of the B_4C(2.5 nm)/[Pd(2 nm)/B_4C(2 nm)/Y(2 nm)]$_{\times40}$/Si sample as well as the zoomed range of interest (intensity in linear scale) are presented in Fig. 2. The Y Kα emission can be observed on the spectrum at photon energy near 15 keV, but due to its low intensity and small estimated angular range for Kossel detection (about 0.5° grazing exit angle, in the total reflection zone), it would not be possible to observe its Kossel oscillation. The energy calibration of the spectrum is carried out with Pd Lα (2.838 keV) and Y Kα (14.958 keV) peaks. Y Lα and Si Kα emissions are not considered because their energies are close to the low energy limit of the camera and their detection is not as efficient as Pd Lα emission. Pd Lβ emission is not discussed either because its intensity is much less than that of the of Pd Lα emission and would not

bring supplementary information. The Pd Lα1 and Lα2 emissions are not resolved, the difference in their energies being less than the detector resolution of about 150 eV at Mn Kα (5.9 keV). A region of interest (ROI) is placed on the spectrum in order to distinguish the Pd Lα emission from other photons, see Fig. 3(a) where the intensity of Pd Lα emission is obtained by integrating the shadowed area. The ROI width of 100 eV is based on a compromise between obtaining good statistics and limiting the influence of the Pd Lβ emission. An image of the spatial distribution of the Pd Lα emission intensity (Fig. 3(b)) is obtained after applying the energy filtering ROI of Fig. 3(a) to the total intensity image presented in Fig. 1. While it is not possible to observe the Kossel feature in Fig. 1, now it can be clearly seen in Fig. 3(b). Finally we integrate this filtered image along the vertical pixels in order to obtain the Kossel curve which is presented in Fig 3(c).

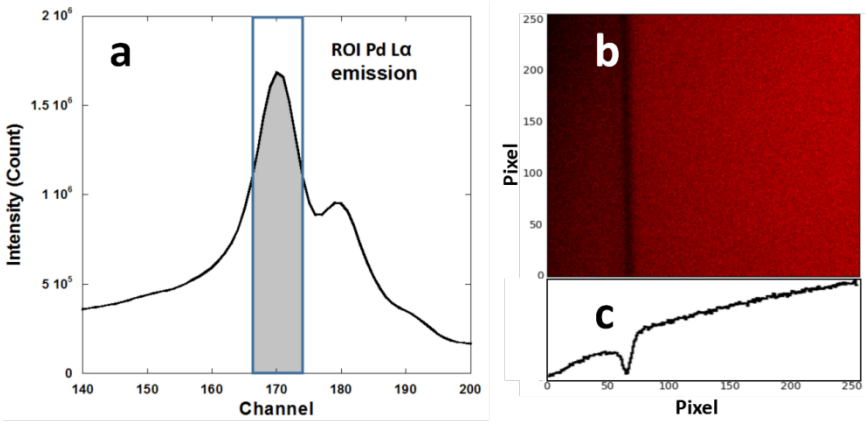

Fig. 3. a) Selection of the ROI for Pd Lα emission; for the case already depicted in Fig. 1: b) image of the intensity of X-ray emission, of which the energy is in the ROI; c) Kossel curve depicted by integrating the X-ray emission intensity along the vertical pixel.

To check the stability of the measurement and possible sample damage from the proton irradiation, we consider the sample B_4C(2.5 nm)/[Pd(2 nm)/B_4C(2 nm)/Y(2 nm)]$_{\times 40}$/Si and continue measuring for over 7 hours. The result is presented in Fig. 4 where the curve intensities are normalized by the proton beam current and the acquisition time. We divide this series of measurements into 4-time slices and depict separately the related Kossel curves of Pd Lα emission to see if any deformation of the Kossel feature happens. The oscillation maintains its shape, indicating that the structure of the multilayer is not changed during the measurement and the proton beam causes no discernible change to the sample structure. We can safely say that the whole experiment is non-damaging because the standard acquisition time for each sample is about 2 hours.

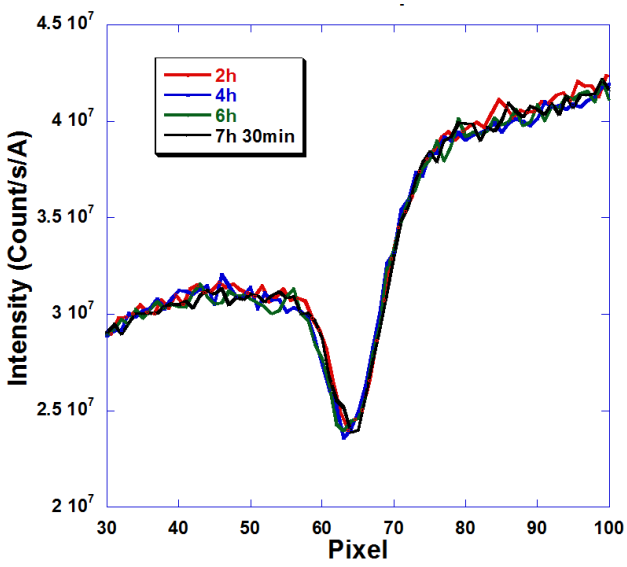

Fig. 4. Non-damaging test of the sample B_4C(2.5 nm)/[Pd(2 nm)/B_4C(2 nm)/Y(2 nm)]$_{\times 40}$/Si.

The relation between the grazing exit angle and the channel in pixel of the detector is determined with the angular variation of Pd Lα emission intensity of the 4-layer sample B_4C(2.5 nm)/[B_4C(1 nm)/Pd(2 nm)/B_4C(1 nm)/Y(2 nm)]$_{\times 20}$/Si where both the first and second orders of the Kossel diffraction can be observed. The calibration method, which is based on the comparison between experimental and simulated Kossel curves, is presented in Fig. 5. The experimental data and its derivative enable us to locate the position of the Kossel oscillation in pixels, which together with the angle of the Kossel oscillation from simulated curve gives 1° equals to 94.42 channel. Thus the angular range of the X-ray color camera is 256/ 94.42 = 2.71°. The simulation method will be presented later.

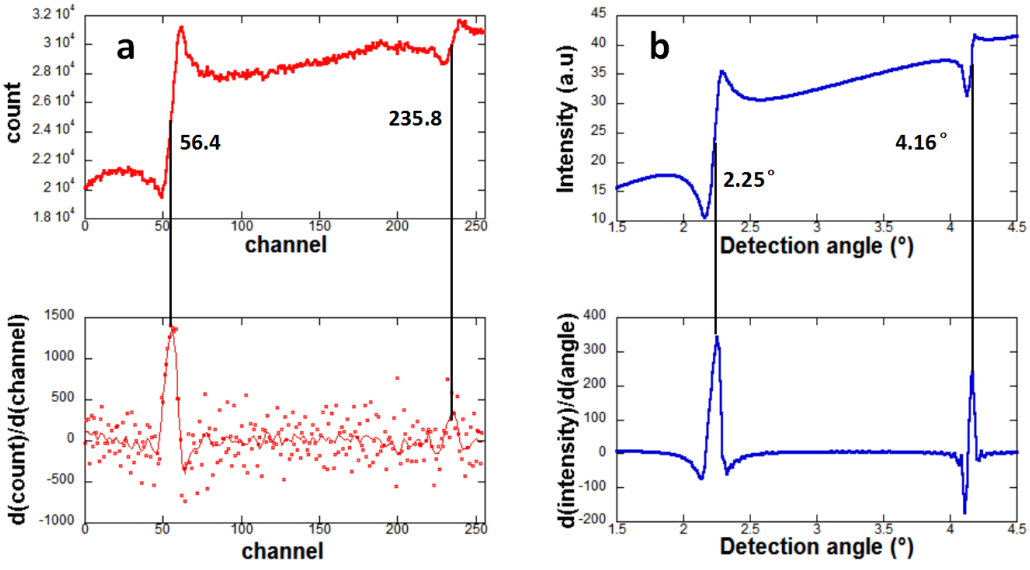

Fig. 5. Calibration of the detection angle using the comparison between a) experimental and b) simulated Kossel curves.

Results and discussion

In Fig. 6 we present the Kossel curves for Pd Lα emission of all measured samples. To facilitate the comparison of the shapes of the curves, for each sample the origin of the detection angle is set to

the Bragg angle, which corresponds to the center of its Kossel oscillation. Fig. 6(a) shows the Kossel curves of the Pd/Y multilayers deposited with a proportion of N_2 within the argon sputtering gas ranging from 0 to 6%. For the Pd/Y multilayer grown in pure argon we observe no Kossel feature at all. This indicates that the intermixing is so severe that even the periodicity of the multilayer is compromised. As the proportion of N_2 increases, we start to observe the Kossel feature and its contrast (defined as the difference between the maximal and minimal intensity values as the detection angle crosses the Bragg angle) increases as well. As expected [21,22], the nitrogen has a positive effect in preventing or reducing the intermixing at the interfaces of the multilayer. Fig. 6(b) presents the Kossel curves of the multilayers with 1 nm B_4C diffusion barriers at one given interface or at both interfaces. The Kossel feature of each sample can be clearly observed. For the two samples with 1 nm B_4C barrier layer inserted at either Y-on-Pd or Pd-on-Y interfaces (noted as B4C/Pd/Y_122 and Pd/B4C/Y_212 respectively), the Kossel features are different when the detection angle is higher than the Bragg angle. The first one exhibits an intensity maximum at +0.05° while the latter shows rather flattened feature at the same angular position. When inserting 1 nm B_4C at both interfaces (the sample labeled as B4C/Pd/B4C/Y_1212), the intensity maximum at +0.05° become even more obvious, however at -0.05° the intensity decrease of the curve is more flattened than the two samples mentioned above. Here we do not present the sample mentioned in the previous section with 2 nm B_4C barrier layer because it is considered expendable for the long-time non-damaging test. Thus it is unsuitable to be put in the comparison series.

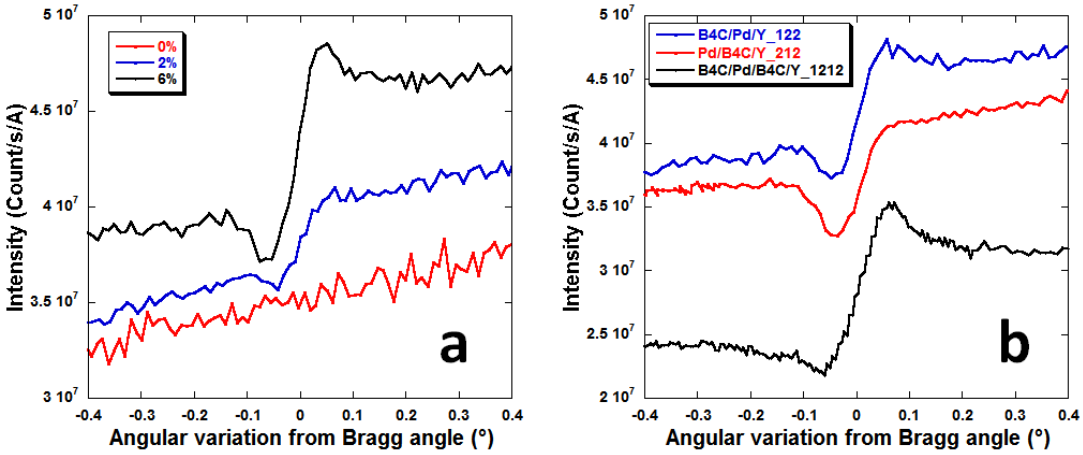

Fig. 6. Kossel curves for Pd Lα emission of all measured samples. a) series of samples fabricated with different concentration of N_2 in the sputtering gas; b) series of samples with B_4C barrier layers at one given interface or at both interfaces. For this latter series, the name of the samples refers both to the order of the layers within the period and to the thickness (in nm) of the individual layers.

To simulate the PIXE-Kossel curve, we build model of the multilayer using the structural parameters (thickness and roughness of the layers) determined by grazing incident X-ray reflectivity. The simulation method is originally designed for X-ray fluorescence calculation under Kossel effect [2]. It calculates the electric field generated by the emitted X-ray within the multilayer under X-ray irradiation. We make an approach in order to adapt it to the PIXE-Kossel calculation. Since the ionization is uniform through the whole multilayer, we consider the incident proton beam as an photon beam with neither attenuation nor refraction. Such approach actually simplifies the calculation. An example of the simulation is given in Fig. 7 where both experimental and simulated the PIXE-Kossel

curves are presented in the near Bragg angle zone. The agreement is fairly good showing that the PIXE-Kossel curve can be used to determine the structure of multilayer stack.

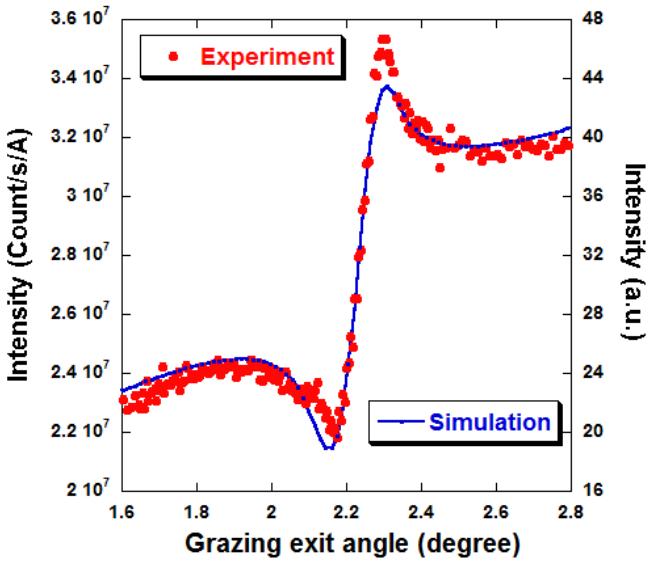

Fig. 7. Comparison between experimental result and simulation of the PIXE-Kossel curves of the sample B_4C(2.5 nm)/[B_4C(1 nm)/Pd(2 nm)/B_4C(1 nm)/Y(2 nm)]$_{\times 20}$/Si.

Conclusion

We have shown the feasibility of using proton induced X-ray emission combined with Kossel diffraction to characterize the structure of nanometric multilayers. We have measured the Kossel diffraction of proton induced Pd L□ emission in Pd/Y based multilayers. Compared to our previous experiment [20], we have significantly improved the data acquisition with the X-ray color camera. We also demonstrate here that the shape of the Kossel curve is very sensitive to the detailed structure of the multilayer and its interface. In particular we confirm that nitridation during the multilayer deposition process has a positive effect in preventing or reducing the interdiffusion between Pd and Y layers, and we further show that Pd/Y based multilayers with B_4C barrier layers at different interfaces can be distinguished by the shape of their Kossel curves.

References

[1] W. Kossel, V. Loeck, H. Voges, Die Richtungsverteilung der in einem Kristall entstandenen charakteristischen Röntgenstrahlung, Z. Für Phys. 94 (1935) 139–144, http://dx.doi.org/10.1007/BF01330803.

[2] J.-P. Chauvineau, F. Bridou, Analyse angulaire de la fluorescence du fer dans une multicouche périodique Fe/C, J. Phys. IV 6 (1996), http://dx.doi.org/ 10.1051/jp4:1996707, C7-53–C7-64.

[3] J.-P. Chauvineau, O. Hainaut, F. Bridou, Lignes de Kossel observées avec des multicouches périodiques Fe/C, J. Phys. IV. 6 (1996), http://dx.doi.org/10.1051/jp4:1996475, C4-773–C4-779.

[4] M.A. Chuev, M.V. Koval'chuk, V.V. Kvardakov, P.G. Medvedev, E.M. Pashaev, I.A. Subbotin, S.N. Yakunin, Direct observation of anomalous Kossel lines, JETP Lett. 91 (2010) 191–195, http://dx.doi.org/10.1134/S0021364010040077.

[5] S. Marchesini, M. Belakhovsky, A.Q.R. Baron, G. Faigel, M. Tegze, P. Kamp, Standing waves and Kossel line patterns in structure determination, Solid State Commun. 105 (1998) 685–687, http://dx.doi.org/10.1016/S0038-1098 (97)10214-9.

[6] C. Schetelich, S. Brenner, V. Geist, Laue and Kossel diffraction on quasicrystals by means of synchrotron radiation, J. Synchrotron Radiat. 5 (1998) 102–106, http://dx.doi.org/10.1107/S0909049597017901.

[7] P. Jonnard, Y.-Y. Yuan, K. Le Guen, J.-M. André, J.-T. Zhu, Z.-S. Wang, F. Bridou, Spontaneous soft X-ray fluorescence from a superlattice under Kossel diffraction conditions, J. Phys. B At. Mol. Opt. Phys. 47 (2014) 165601, http:// dx.doi.org/10.1088/0953-4075/47/16/165601.

[8] Y. Tu, Y. Yuan, K. Le Guen, J.-M. André, J. Zhu, Z. Wang, F. Bridou, A. Giglia, P. Jonnard, X-ray fluorescence induced by standing waves in the grazing-incidence and grazing-exit modes: study of the Mg–Co–Zr system, J. Synchrotron Radiat. 22 (2015) 1419–1425, http://dx.doi.org/10.1107/ S1600577515016239.

[9] V.V. Lider, X-ray divergent-beam (Kossel) technique: a review, Crystallogr. Rep. 56 (2011) 169–189, http://dx.doi.org/10.1134/S106377451102012X.

[10] P. Jonnard, J.-M. André, C. Bonnelle, F. Bridou, B. Pardo, Modulation of X-ray line intensity emitted by a periodic structure under electron excitation, Appl. Phys. Lett. 81 (2002) 1524–1526, http://dx.doi.org/10.1063/1.1502189.

[11] P. Jonnard, J.-M. André, C. Bonnelle, F. Bridou, B. Pardo, Soft-X-ray Kossel structures from W/C multilayers under various electron ionization conditions, Phys. Rev. A 68 (2003) 32505, http://dx.doi.org/10.1103/PhysRevA.68.032505.

[12] J.-M. André, P. Jonnard, B. Pardo, Radiation emitted by an oscillating dipole embedded in a periodic stratified structure: a direct matrix analysis, Phys. Rev. A 70 (2004) 12503, http://dx.doi.org/10.1103/PhysRevA.70.012503.

[13] V. Geist, R. Flagmeyer, The influence of the crystal lattice on the angular distribution of X-rays emitted from a GaP single crystal by fast proton bombardment, Phys. Status Solidi A 26 (1974) K1–K3, http://dx.doi.org/ 10.1002/pssa.2210260141.

[14] J.B. Roberto, B.W. Batterman, V.O. Kostroun, B.R. Appleton, Positive ion induced Kossel lines in copper, J. Appl. Phys. 46 (1975) 936– 937, http://dx.doi.org/10.1063/1.321618.

[15] V. Geist, R. Flagmeyer, D. Stephan, H.-J. Ullrich, Kossel interferences of proton-induced Al Ka radiation, Phys. Status Solidi A 40 (1977) 113–117, http://dx. doi.org/10.1002/pssa.2210400115.

[16] V. Geist, R. Flagmeyer, G. Otto, Investigation of lattice deformation in proton bombarded GaP and ZnSiP2 by means of the proton-induced kossel effect, Phys. Lett. A 64 (1978) 421–422, http://dx.doi.org/10.1016/0375-9601(78) 90288-8.

[17] V. Geist, C.H. Ehrlich, R. Flagmeyer, H.J. Ullrich, W. Greiner, S. Rolle, Investigation of GaN heteroepitaxial layers by means of the kossel effect technique, Cryst. Res. Technol. 17 (1982) 245–251, http://dx.doi.org/ 10.1002/crat.2170170218.

[18] J. Rickards, Crystallography using the diffraction of proton induced X-rays, Nucl. Instr. Meth. Phys. Res. Sect. B Beam Interact. Mater. At. 24 (1987) 621– 624, http://dx.doi.org/10.1016/S0168-583X(87)80210-0.

[19] C. Schetelich, S. Weber, V. Geist, M. Schlaubitz, H.J. Ullrich, S. Kek, H.G. Krane, Recording of Kossel patterns using monochromatic synchrotron radiation, Nucl. Instr. Meth. Phys. Res. Sect. B Beam Interact. Mater. At. 103 (1995) 236– 242, http://dx.doi.org/10.1016/0168-583X(95)00594-3.

[20] M. Wu, K. Le Guen, J.-M. André, V. Ilakovac, I. Vickridge, D. Schmaus, E. Briand, S. Steydli, C. Burcklen, F. Bridou, E. Meltchakov, S. de Rossi, F. Delmotte, P. Jonnard, Kossel interferences

of proton-induced X-ray emission lines in periodic multilayers, Nucl. Instr. Meth. Phys. Res. Sect. B: Beam Interact. Mater. At. 386 (2016) 39–43, https://doi.org/10.1016/j.nimb.2016.09.014.

[21] D. Xu, Q. Huang, Y. Wang, P. Li, M. Wen, P. Jonnard, A. Giglia, I.V. Kozhevnikov, K. Wang, Z. Zhang, Z. Wang, Enhancement of soft X-ray reflectivity and interface stability in nitridated Pd/Y multilayer mirrors, Opt. Express. 23 (2015) 33018, https://doi.org/10.1364/OE.23.033018.

[22] M.-Y. Wu, V. Ilakovac, J.-M. André, K. Le Guen, A. Giglia, J.-P. Rueff, Q.-S. Huang, Z.-S. Wang, P. Jonnard, Study of Pd/Y based multilayers using high energy photoemission spectroscopy combined with x-ray standing waves, SPIE Proc. (2017) 102350F, https://doi.org/10.1117/12.2265630.

[23] M. Prasciolu, A.F.G. Leontowich, K.R. Beyerlein, S. Bajt, Thermal stability studies of short period Sc/Cr and Sc/B_4C/Cr multilayers, Appl. Opt. 53 (2014) 2126, https://doi.org/10.1364/AO.53.002126.